Pergamon

Tetrahedron: *Asymmetry* 9 (1998) 2259–2270

TETRAHEDRON: *ASYMMETRY*

Rhodium dihydride complexes as models for the theoretical analysis of enantioselective hydrogenation reactions

Gheorghe Surpateanu,[a,*] Francine Agbossou,[b,*] Jean-François Carpentier[b] and André Mortreux[b]

[a]*Laboratoire de Synthèse Organique et Environnement, Maison de la Recherche en Environnement, Université du Littoral, 145 Route du Pertuis d'Amont, 59140 Dunkerque, France*

[b]*Laboratoire de Catalyse Hétérogène et Homogène, URA CNRS 402, ENSCL, BP 108, 59652 Villeneuve d'Ascq Cedex, France*

Received 1 April 1998; accepted 9 June 1998

Abstract

A combination of molecular mechanics methods and extended Hückel calculations has been applied in order to have access to the more stable complexes expected to be involved as catalytic intermediates in the enantioselective hydrogenation of ketopantolactone (KPL) using chiral aminophosphine-phosphinite (AMPP) chlororhodium complexes. The product selectivity has been deduced from correlations between the prevailing configuration of the hydrogenated derivatives and the energetics of competing diastereomeric dihydride complexes of formula $[RhCl(H)_2(AMPP)(KPL)]$ with the assumption that the enantioselectivity is controlled by the relative energies of such intermediates. The calculations have been obtained from the application of sequential and exhaustive search methodologies. The procedure has been applied to complexes bearing the aminophosphine-phosphinites (*S*)-Cp,Cp-ProNOP (**IV**) and (*S*)-Ph,Cp-ProNOP (**V**) and bis(aminophosphanes) derived from 2-(anilinomethyl)pyrrolidine (**VI–IX**). The latter induce a reversal of configuration of the major enantiomer of the hydrogenation product when varying specific substituents at the phosphorus atoms. Computations were carried out also for complexes bearing the two enantiomers (*S*)- and (*R*)-Ph,Cp-isoAlaNOP. The lowest energy complexes present enantiomeric structures. A novel insight into the local reactivity of the intermediates has been gained from determining the first migrating hydride according to the superdelocalizability parameter calculated for all isomers. Thus, the configurations of pantolactone arising from the alkoxyrhodium species obtained when assuming a nucleophilic attack of one of the hydrides to the carbonyl group of the ketone has been defined and are in total agreement with the experimental data.

* Corresponding authors. E-mail: surpatea@univ-littoral.fr and agbossou@ensc-lille.fr

0957-4166/98/$ - see front matter
PII: S0957-4166(98)00226-2

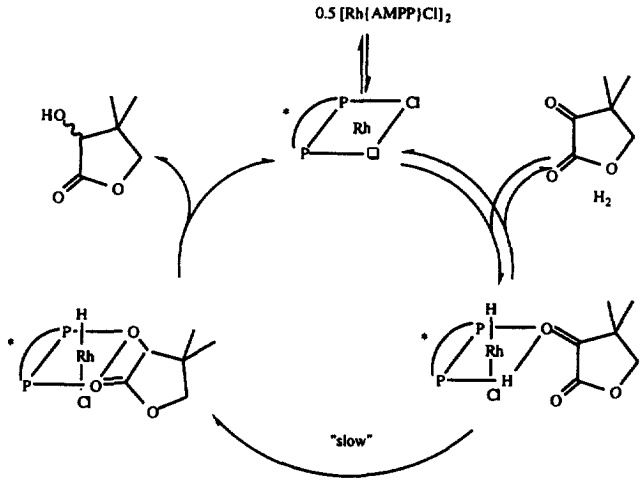

Fig. 1. Proposed mechanism for the hydrogenation of KPL[5]

1. Introduction

We have reported recently a comparative study between experimental results and a theoretical analysis relative to the enantioselective hydrogenation of prochiral ketones promoted by rhodium-AMPP complexes (AMPP: aminophosphine-phosphinite).[1] Our initial approach in looking for the origins of product selectivity was based on molecular mechanics and extended Hückel calculations of rhodium dihydride model complexes of general formula $[RhCl(H)_2(AMPP)(KPL)]$ expected to be involved in both the kinetic and enantioselective steps of the catalytic cycle (Fig. 1).[2] Although dihydride complexes, assumed to be produced via the oxidative addition of H_2 onto the substrate–catalyst adduct,[3] are the commonly accepted intermediates in transition metal-catalysed homogeneous hydrogenations, they had not been observed until very recently. Indeed, the PHIP-NMR technique (PHIP: parahydrogen-induced polarisation) allowed the identification of such species in the rhodium-based asymmetric hydrogenation of dimethyl itaconate.[4] That technique has also been employed to obtain kinetic data for the enantioselective hydrogenation of ethyl (*Z*)-α-acetamidocinnamate using $[Rh(NBD)(chiraphos)]BF_4$ as the catalyst.[5] The specific occurrence of polarisation in the ^1H NMR spectra results from a pairwise transfer of hydrogen to the substrate. That observation is consistent with the prior addition of molecular hydrogen to the rhodium complex followed by a rapid transfer of both hydrides to the bound substrate.

In the case of the above prochiral ketone hydrogenation (Fig. 1), we correlated the enantioselection with the energetics of competing diastereomeric dihydride intermediates and we could correctly predict the configuration of the prevailing alcohol when assuming the most stable adducts providing the observed hydroxy compounds.[1] Evidently, our hypothesis does not exclude a prior competition between transition states under kinetic control. In fact, the sequence of the kinetically relevant steps that has been defined for the cationic rhodium based enantioselective hydrogenation of prochiral enamides cannot be extended with certainty to the hydrogenation of ketones accomplished in the presence of neutral rhodium catalysts. Thus, examination of the energetics of six coordinate dihydride complexes has been taken as a crude probe of transition models. The latter can account for the enantiocontrolled step of the hydrogenation. The 'calculated' configurations have been deduced from the insertion of one of the hydrides into the coordinated *si* or *re* ketone which constitutes a different approach from the correlation carried out earlier for the enantioseletive hydrogenation of dehydroamino acids.[6]

The substance of our study was provided by the uncommon hydrogenation feature (i.e. the reversal

of the configuration of the major hydrogenation product) induced by ligands differing only in the substituents born by their phosphorus moieties. Nevertheless, such a trend is not general and only a few other AMPPs exhibit that peculiar behaviour. Consequently, the latter appear also to be excellent prospects for further calculations. Accordingly, we sought to extend the calculations to those bisphosphines as well. Here, we wish to report the results of new computations that have been carried out with the aim of reinforcing our strategy in the molecular modelling of the hexacoordinate dihydride isomers using sequential and exhaustive search methodologies. Also, a novel insight into the local reactivity of the dihydride-intermediates has been gained from viewing the isovalued surface of the molecular electron density. Thus, the assumed preferred migrating hydride, which we take as responsible for the stereochemical course of the reaction in the hydride-transfer step, was conveniently deduced from molecular superdelocalizability data as detailed below.

2. Methodology

2.1. New systems investigated

As mentioned above, for our previous study, we selected Rh-AMPP based catalytic systems which exhibit a singular behaviour i.e. a reversal of the configuration of the prevailing enantiomer by just varying substituents at the phosphorus moieties of the ligands.[7] As a matter of fact, the involvement of the dinuclear chlororhodium complex of (*S*)-Cp,Cp-isoAlaNOP (Cp=cyclopentyl) (designed afterwards as system **I**) afforded the *S* enantiomer of pantolactone in 89% enantiomeric excess (ee) while the corresponding (*S*)-Ph,Cp-isoAlaNOP catalyst (**II**) led to 81% ee in the *R* enantiomer (Table 1, Scheme 1).[7a] Interestingly, this phenomenon is not observed with the closely related ProNOP systems (**IV** and **V**),[7a] but is still present in the ProNN′P family (**VI–VIII**) (Table 1).[6b]

Our goal here is first to validate our modelling procedure and bring improvements to the conformational search and secondly to look closer at the reactivity of the complexes in order to define the first migrating hydride. Accordingly, we applied a new thorough minimization procedure (1) to previously reported structures derived from systems **I** and **II** for comparison between the two methodologies, (2) to two complexes bearing enantiomeric ligands, and (3) to both the ProNOP and ProNN′P based systems **IV–IX** (Table 1, Scheme 1). Furthermore, the electron density isosurface, computed in order to visualise a specific electronic property of the complexes i.e. the electrophilic superdelocalizability, has been calculated for all adducts **I–IX**.

2.2. Molecular modelling of dihydride structures

In this part, we present, in detail, the new methodology taking as examples the new systems investigated. For each system **IV–IX**, different dihydride isomeric structures of general formula [RhCl(H)$_2$(AMPP)(KPL)] were investigated according to the respective position of the ligands at the square planar and the apical sites i.e. diphosphine, ketopantolactone, chloride and hydrides. As the more appropriate binding arrangements have been deduced from our previous investigations, the present study has been restricted to the hexacoordinate dihydride structures in which KPL is coordinated in the square plane (trans to one phosphine residue). Indeed, the six other possible dihydride structures having the ketone at an apical site (with respect to the RhP$_2$ square plane) were systematically found to be much less stable.[1] In fact, the selected isomers **1**, **2**, **4**, and **5** correspond to different cis dihydrides that can be considered as the result of cis addition of molecular hydrogen to the rhodium from different

Table 1
Selected systems and corresponding experimental results for the rhodium-based asymmetric hydrogenation of ketopantolactone[a]

System	Diphosphine P_2*	ee (config.)[b]
I	(*S*)-Cp,Cp-isoAlaNOP	89 (*S*)
II	(*S*)-Ph,Cp-isoAlaNOP[c]	81 (*R*)
III	(*R*)-Ph,Cp-isoAlaNOP	81 (*S*)
IV	(*S*)-Cp,Cp-ProNOP	75 (*R*)
V	(*S*)-Ph,Cp-ProNOP	85 (*R*)
VI	(*S*)-Cp,Cp-ProNN'P	70 (*S*)
VII	(*S*)-Ph,Ph-ProNN'P	33 (*R*)
VIII	(*S*)-Cp,Ph-ProNN'P	80 (*S*)
IX	(*S*)-Ph,Cp-ProNN'P	nd[d]

[a]See reference 1. [b]Enantiomeric excesses and absolute configuration of the prevailing enantiomer of pantolactone. [c]The (*S*)-Ph,Ph-isoAlaNOP gave the *R* hydrogenated product with 11% ee. [d]Experimental result not available due to the present inaccessibility of the ligand. This ligand should give the (*S*) product according to our calculations (see Table 2).

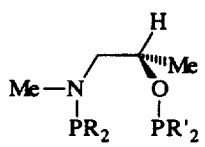

(*S*)-R,R'-isoAlaNOP

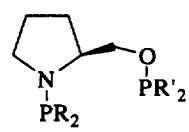

(*S*)-R,R'-ProNOP

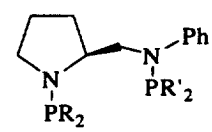

(*S*)-R,R'-ProNN'P

R, R' = Ph, Cp (cyclopentyl)

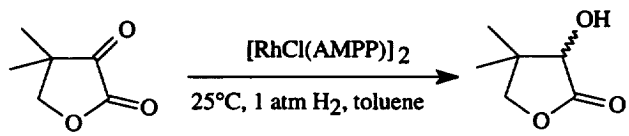

Scheme 1.

trajectories. Trans dihydrides **3** and **6** were also considered. Furthermore, based on the most stable geometries, the starting conformation of the seven membered chelate used in the selected structures

is a twist-boat with the non cyclic oxygen (or nitrogen) atom lying in the plane defined by P–Rh–P. However, that conformation is not held rigidly during the calculations. The schematic description of the six selected isomers for each system and the labelling of the hydridic sites are sketched in Schemes 2 and 3 respectively.

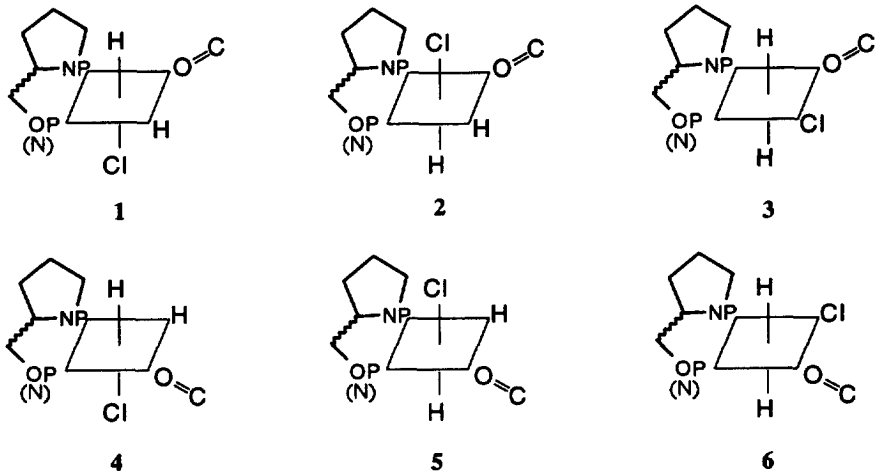

Scheme 2.

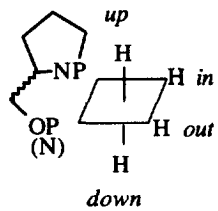

Scheme 3.

Molecular modelling of these structures was carried out using an iterative combination of molecular mechanics and extended Hückel computations as implemented in the CAChe Worksystem 3.9. The force field model used for the molecular mechanics minimizations is augmented MM2 with modifications and additions to the parameter set as described earlier.[1] Namely, adjustment of the force constants and interatomic distances for the bonds to rhodium have been made.[8] Extended Hückel calculations were performed by using the standard STO-3G basis set, a Wolfberg–Helmholtz constant K of 1.75, and the experimentally-based EHT parameters.

Thus, each selected structure was generated by molecular graphics and the conformation space was searched following the new low-energy pathway described herein. Each of the six generated structures for each new system (**IV–IX**) (36 structures total) was subjected to 1300 steps of energy minimization using the conjugate gradient and the block diagonal Newton–Raphson algorithm (0.001 kcal/mol convergence for each technique). These two techniques were applied back and forth until a threshold of 0.001 kcal/mol.

Next, each lowest energy structure was used as the starting point for a multipass multiple conformer sequential search. The main degrees of conformational flexibility appeared to be rotation about 4 P–C and the Rh–O bonds. Accordingly, these torsions define the potential energy grid to be searched. The 5 corresponding torsions were defined and traversed in sequence during the sequential search, the last being the Rh–O bond (Fig. 2). We did not consider the rotation around the N–Ph bond for this step of minimisation as we checked that the rotation of the latter did not influence at all the energy and the

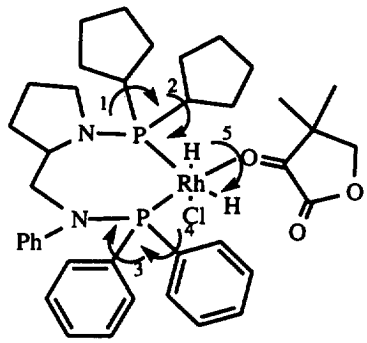

Fig. 2. Sequence of torsion angle definitions (from 1 to 5, schematised by the arrows). System **VIII.1** is taken as an example for the labelling

structure of the most stable conformers. However, it is interesting to mention that calculations carried out with a sp^3 configuration for the nitrogen atom gave structures that were more stable than with a sp^2 nitrogen configuration.

For each search, the torsion angle was advanced systematically in 15° increments through 360°. The lowest energy conformer resulting from each multiconformer search provides the starting structure for the following calculations. Indeed, the next computation involved the rotation around all the 5 previously defined single bonds taken one by one in the same sequence as defined above. The procedure started with the first torsion (24 steps of 15°) for which an exhaustive optimized potential energy map was computed using both procedures as described above. As a result, the diagram obtained displays the steric energy versus the torsion angle and is composed by the assemblage of the explored conformations including the most stable one. The extended Hückel energy is then computed for each molecular conformation of the assemblage and a new diagram total energy versus the torsion angle is achieved with a profile that can be different.

The lowest energy structure is selected and the complete set of calculations is renewed while rotating the second torsion angle of the sequence. The same procedure is applied until all 5 bonds were rotated. From that complete study, only the conformer of lowest global energy is retained as the minimum.

2.3. *Determination of the first migrating hydride*

The configuration of a hydrogenated product is the result of the migratory insertion step involving one of the hydrides and the *si* or *re* face of the bound substrate. It is commonly accepted[9] that the latter proceeds via the nucleophilic attack of the H atom to the carbonyl C atom of the coordinated ketone yielding an alkoxy–rhodium species. Therefore, the designation of the most reactive hydrogen atom of the dihydride intermediate towards the electrophilic carbon can be made, as reported earlier, by estimating the respective hydridic character (partial charge combined with the distance between the two reacting centres).[1]

Another approach is to locate the site of the complex susceptible to an external 'electrophilic attack' which is evidently expected at one of the hydrides. Such information is also gained when using the molecular electrophilic superdelocalizability $s(x)_E$ parameter. Molecular superdelocalizabilities, s, were defined by Fukui et al.[10] using an equation in the form of Eq. 1.

$$s(x) = \sum_{i=1}^{N} \frac{(\nu_i - \nu)\phi_i(x)^2}{\alpha - E_i}(-\beta) \tag{1}$$

The $s(x)$ parameter is the superdelocalizability at point x, N is the total number of orbitals, $\phi_i(x)$ is the value of the filled orbital i at point x and E_i is the energy of that orbital in electron volts (eV). The summations are over all occupied and all empty orbitals, respectively. The v_i parameter is the number of electrons in orbital i and is usually 0, 1, or 2. Parameter v is the number indicating the type of reaction and is 0 for an electrophilic reaction. Parameter β is the interaction energy between reagent and substrate atomic orbitals and α is the reagent energy.

The electrophilic superdelocalizability data is computed from the electron density isosurface of the complexes which reveals the reactive sites based on the electron distribution of frontier orbitals. In order to perform the calculation, the choice of the energy, α, of a hypothetical reagent is critical. The best values are in between the HOMO and LUMO energies of the adducts and they approximate the energy of the frontier orbital. A typical value, which proved suitable afterwards for our computations, is -8 eV. The $s(x)_E$ parameter has been determined for all complexes **I–IX**.

3. Results and discussion

In order to provide a context for the results obtained during this study, relevant selected previous data for systems **I–III** are summarized first in Table 2 followed by the key data of the computations carried out for systems **IV–IX**. All data are selected according to the lowest total energy of the complexes. When looking carefully at the corresponding structures, we notice that, despite coordinate randomization in the modelling process, the computed dihydride complexes exhibit rather small distortions from an ideal octahedral geometry. Furthermore, the bond distances around rhodium do not vary much from one structure to the other and are usually quite similar to initial requirements. In particular, the lengthening of the Rh–P bond trans to the hydride suggested by NMR coupling data[3] and previous computations[11] was not observed during our computations.

As mentioned above, the complete new pathway of minimization has been applied to the two previously analyzed systems i.e. **I.2** and **II.1** (Scheme 1, Table 1). For system **I.2**, the difference of total energy between the two minimization procedures is 0.06 kcal/mol, the new strategy giving the lowest energy. For system **II.1**, the opposite is observed. Namely, the difference of energy is 0.53 kcal/mol, the previously minimized structure presenting the lowest energy. The two computations lead to very similar structures and the resulting geometries are almost identical when comparing the two strategies. Calculations have also been carried out on complexes bearing the two enantiomers of Ph,Cp-isoAlaNOP. In particular systems **II.1** and **III.2** are the most stable with a difference in total energy of 0.02 kcal/mol. As expected, the two complexes are enantiomers as illustrated in Fig. 3. These results make us question the reliability of the computations when it comes to the use of the energetic differences for a quantitative evaluation of the enantioselectivities. When looking at the energy difference of both minimized structures **II.1** and **III.2** bearing enantiomeric ligands (ΔE=0.02 kcal/mol), we could be tempted to conclude that there is a good level of refinement. However, the real level of energy discrimination is certainly higher and dependent on the procedure applied for the minimization (compare structures **I.2** and **II.1**).

Except for **VII**, the new systems investigated present the chlorine atom in an apical position for the most stable isomeric geometries (structures **1**, **2**, **4** and **5**; Scheme 2). Accordingly, they exhibit the cis-dihydride arrangement which is consistent with a cis-oxidative addition process of H_2[12] and with recent NMR data.[3] All structures appear to be driven by minimization of steric interactions between the geminate dimethyl moiety of KPL with the surrounding complex. Interestingly, the general conformation and geometry of the chiral backbone remains quite constant for one family of complexes. Thus, it is the way the coordinated ketone satisfies the minimization of steric interactions that defines the preferentially

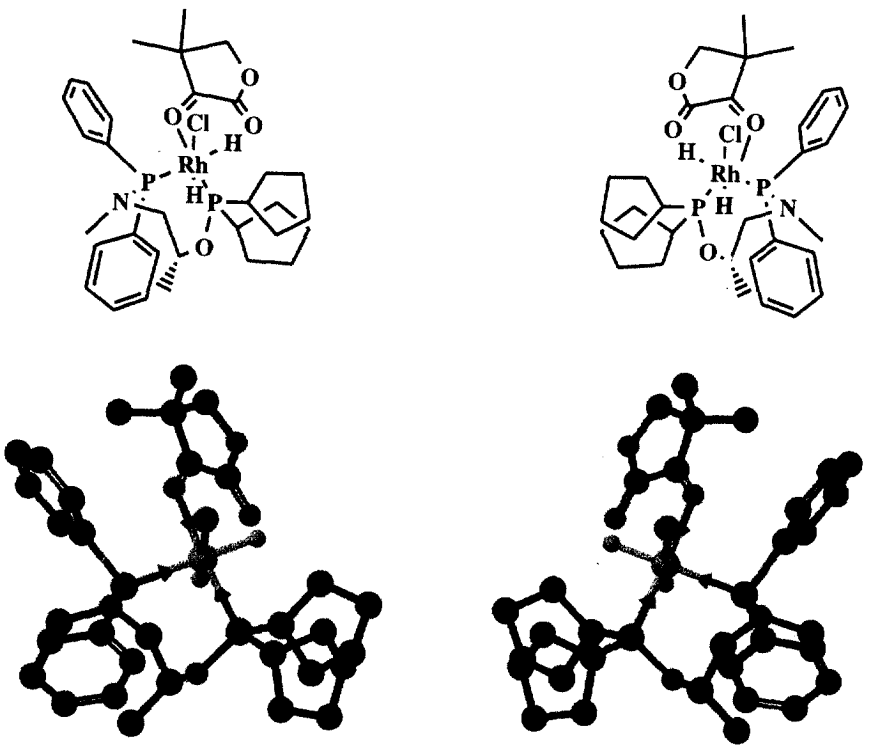

Fig. 3. Lowest energy structure for the system [RhCl(H)$_2$(KPL){(*R*)-Ph,Cp-isoAlaNOP}] (left) and [RhCl(H)$_2$(KPL){(*S*)-Ph,Cp-isoAlaNOP}] (right)

Table 2
Main characteristics of lowest total energy six-coordinate dihydride structures

system[a]	total energy[b] (au)	ΔE[c] (kcal/mol)	hydride type[d]	partial charge	d (H...C) (Å)[e]	$s(x)_E$	result. config.[f]
I.3	-138.014	0	d	-0.70	3.20	0.302	*R>S*
			u	-0.69	3.31	0.295	
I.2	-138.013	0.6	o	-0.73	2.75	0.332	*S*
			d	-0.65	3.05	0.288	
I.1	-138.002	7.6	o	-0.71	2.68	0.332	*R*
			u	-0.62	3.36	0.283	
II.1	-137.702	0	o	-0.72	2.87	0.320	*R*
			u	-0.63	3.38	0.280	
II.3	-137.699	2.1	u	-0.68	3.52	0.292	*R>S*
			d	-0.69	3.35	0.297	
II.2	-137.696	3.8	o	-0.72	2.99	0.325	*R*
			d	-0.66	3.18	0.290	
III.2	-137.705	0	o	-0.72	2.71	0.323	*S*
			d	-0.64	3.17	0.285	
III.2'	-137.701	2.5	o	-0.71	2.82	0.323	*R*
			d	-0.64	3.02	0.285	
III.3	-137.697	5.1	d	-0.69	3.17	0.297	*R>S*
			u	-0.69	3.40	0.293	
IV.1	-140.268	0	o	-0.73	3.11	0.341	*R*
			u	-0.63	3.54	0.281	
IV.2	-140.263	3.0	o	-0.73	3.10	0.337	*R*
			d	-0.63	3.14	0.286	
IV.5	-140.263	3.4	i	-0.73	3.13	0.349	*S>R*
			d	-0.63	3.59	0.280	

V.2	-139.978	0	o	-0.71	3.06	0.322	*R*
			d	-0.63	3.22	0.284	
V.1	-139.950	17.3	o	-0.73	3.20	0.331	*S*
			u	-0.63	3.11	0.285	
VI.1	-156.619	0	o	-0.74	3.21	0.342	*S*
			u	-0.63	3.03	0.283	
VI.5	-156.615	2.5	i	-0.73	3.20	0.346	*R*
			d	-0.63	3.32	0.285	
VI.2	-156.606	8.3	o	-0.72	3.15	0.338	*R*
			d	-0.64	3.18	0.283	
VII.3	-155.997	0	u	-0.69	3.55	0.300	*R>S*
			d	-0.70	3.55	0.306	
VII.5	-155.993	2.2	i	-0.70	3.16	0.332	*R*
			d	-0.62	3.39	0.284	
VII.4	-155.987	6.1	i	-0.71	3.21	0.338	*S*
			u	-0.63	3.41	0.280	
VIII.1	-156.305	0	o	-0.73	3.14	0.341	*S*
			u	-0.64	3.08	0.283	
VIII.2	-156.300	3.4	o	-0.72	3.07	0.339	*R*
			d	-0.63	3.45	0.283	
VIII.5	-156.296	5.7	i	-0.70	3.15	0.337	*R>S*
			d	-0.63	3.51	0.287	
IX.1	-156.295	0	o	-0.70	3.13	0.328	*S*
			u	-0.62	3.35	0.282	
IX.4	-156.289	3.8	i	-0.71	3.12	0.356	*S>R*
			u	-0.62	3.44	0.283	
IX.3	-156.286	5.6	d	-0.62	3.00	0.300	*S>R*
			u	-0.62	3.96	0.301	

[a]Lowest energy structures among the six possibilities depicted in Scheme 2. [b]The value of the energy has been corrected to the nearest decimal. [c]The difference of energy has been obtained by using the value of the total energy as computed without the correction mentioned in *c*. [d]d: down, i: in, u: up, o: out, see Scheme 3. [e]The distance reported is the straight interatomic distance between the hydride and the C atom of the coordinated ketone. [f]The configuration of the hydroxy compound reported is the result of the addition of the considered hydride to the coordinated carbonyl of the ketone. When the face of addition is undetermined due to the geometry of the complex, two configurations are given with a preference for the one reported first.

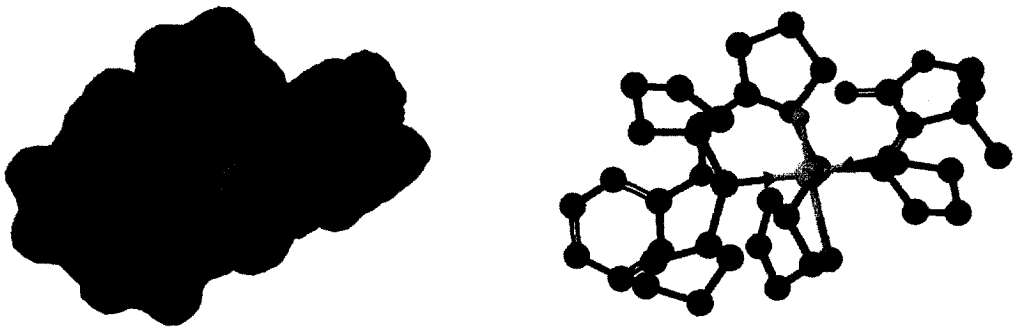

Fig. 4. Newman-type views (along the H*out*–Rh–P bonds) of the electron density isosurface of **VI.1** coloured by electrophilic delocalizability (left) and the corresponding molecular model (right)

bound *si* or *re* enantioface of the carbonyl function. Moreover, it is noteworthy that in the lowest energy structures of aminophosphine-phosphinite systems **IV** and **V**, ketopantolactone is coordinated trans to the Rh–P(O) bond, and consequently a hydride is located trans to the Rh–P(N) bond. This feature is in close connection with our previous proposals assuming that such an arrangement might be a function of the relative acidity of the phosphorus moieties coordinated to rhodium.[5] The sole exception to this trend arises from system **VII** which provides a trans-dihydride arrangement, as previously found for system **I** (vide infra).

In displaying the isovalued surfaces of the assemblies according to the electrophilic superdelocalizability, we found that the equatorial hydrogen atom was designated systematically as the preferred location of an electrophilic attack ($s(x)_E$, Table 2, Fig. 4). Accordingly, that specific hydride can be considered as the more nucleophilic site of the complexes. Thus, it is not unreasonable to extend the concept and consider the latter as migrating in the corresponding insertion step.

Interestingly, for all the systems studied **I–IX**, this criterion is consistent with the relative hydridic character of the same hydrogen atom as defined earlier.[1] Chatt et al. already showed many years ago that the hydrogen which is in the trans position to phosphorus is expected to be much more reactive than the hydrogen in the trans position to chlorine.[13] In the cases of systems **I** and **VII**, which present a trans-dihydride structure, one can notice that the $s(x)_E$ data are much more in favour of the equatorial H atom of the cis-dihydride structure than either of the H atoms present in the lowest energy of the trans-dihydride structure ($s(x)_E$=0.332 versus 0.302, and 0.332 versus 0.300, respectively). Also, the energy difference between the lowest energy trans-dihydride and the immediately following cis-dihydride structures is 0.6 and 2.2 kcal/mol, respectively, and could be even lower if referring to the accuracy of the calculations (vide supra). Therefore it seems reasonable to consider for each system only the lowest energy cis-dihydride arrangement. It could be tempting to rationalise the differences between systems **VII.3** and **VIII.1** taking into account both the magnitude and the sense of the selectivity. However, the resulting correlation would be rather hazardous at this stage of development because of the possible participation of several factors which are not understood (the effect of the catalytic conditions on the order of the kinetic and enantioselective steps i.e. 50°C and 50 bar of H_2 for **VII.3** and 20°C and 1 bar of H_2 for **VIII.1**. Is there a possible isomerisation of a cis-dihydride into a trans-dihydride?).

The definition of the migrating hydride and of the enantioface binding of the ketone enables us to assess the configuration of the prevailing enantiomer of pantolactone (Table 2). However, at this stage of development, the prediction of the magnitude of an asymmetric induction is an impossible task. Indeed, when comparing the configurations in Tables 1 and 2, a total qualitative agreement is observed between the experimental and calculated data thus reinforcing the validity of this simple model. However, to

obtain a correct estimation of the enantiomeric excesses, it is necessary to do the calculations at a suitable level. For that purpose, the use of more accurate calculations (ab initio) could be very helpful. Here, we used EHT but did not obtain correct estimations for the ee's this was attributed to rough computations. Nevertheless, because of the size of the assemblies such a determination represents a difficult task and we hope that it will become possible in the future. The basic findings reported herein, i.e. the involvement of hexacoordinate cis-dihydride structures with ketone coordinated in the square plane as the most important intermediate, will be used in future spectroscopic and computation studies.

Acknowledgements

We thank the 'Ministère de la Recherche et de la Technologie' and the CNRS for their financial support.

References

1. Agbossou, F.; Carpentier, J.-F.; Mortreux, A.; Surpateanu, G.; Welch, A. J. *New J. Chem.*, **1996**, *20*, 1047.
2. Hatat, C.; Karim, A.; Kokel, N.; Mortreux, A.; Petit, F. *New J. Chem.* **1990**, *14*, 141.
3. Landis, C. R.; Halpern, J. *J. Am. Chem. Soc.* **1987**, *109*, 1746.
4. Harthun, A.; Kadyrov, R.; Selke, R.; Bargon, J. *Angew. Chem. Int. Ed. Engl.* **1997**, *36*, 1103.
5. Chinn, M. S.; Eisenberg, R. *J. Am. Chem. Soc.* **1992**, *114*, 1908.
6. (a) Dang, T. P.; Kagan, H. B. *Chem. Comm.* **1971**, 481. (b) Kagan, H. B.; Dang, T. P. *J. Am. Chem. Soc.* **1972**, *94*, 6429. (c) Pavlov, V. A.; Klabunovskii, E. I.; Struchkov, Y. T.; Voloboev, A. A.; Yanovsky, A. I. *J. Mol. Cat.* **1988**, *44*, 217. (d) Knowles, W. S.; Vineyard, B. D.; Sasacky, M. J.; Stults, B. R. *Fundamental Research in Homogeneous Catalysis*, Tsutsui, M. (Ed.); Plenum: New York, 1979, Vol. 3, p. 537.
7. (a) Roucoux, A.; Thieffry, L.; Carpentier, J.-F.; Devocelle, M.; Méliet, C.; Agbossou, F.; Mortreux, A.; Welch, A. J. *Organometallics*, **1996**, *15*, 2440. (b) Roucoux, A.; Suisse, I.; Devocelle, M.; Carpentier, J.-F.; Agbossou, F.; Mortreux, A. *Tetrahedron: Asymmetry* **1996**, *7*, 379.
8. Added parameters for augmented MM2 force field: Rh–Cl, K_s=4.4 mdyn/Å, r_0=2.374 Å; Rh–H, K_s=4.4 mdyn/Å, r_0=1.585 Å; Rh–P, K_s=4.4 mdyn/Å, r_0=2.285 Å; Rh–O, K_s=4.4 mdyn/Å, r_0=2.200 Å.
9. Chaloner, P. A., *Handbook of Coordination Catalysis in Organic Chemistry*, Butterworths, London, 1986, pp. 96–97.
10. (a) Fukui, K.; Yonezawa, T.; Nagata, C. *Bull. Chem. Soc. Jpn* **1954**, *27*, 426. (b) *ibid*, *J. Chem. Phys.* **1957**, *26*, 831.
11. Giovannetti, J. S.; Kelly, M. C.; Landis, C. R. *J. Am. Chem. Soc.* **1993**, *115*, 4040.
12. Collman, J. P.; Hegedus, L. S.; Norton, J. R.; Finke, R. G., *Principles and Applications of Organotransition Metal Chemistry*, University Science Books, Ed.; Mill Valley, CA, 1987, p. 289.
13. Chatt, J.; Coffrey, R. S.; Shaw, B. L. *J. Chem. Soc.* **1965**, 7391.